Desalination and Water Treatment
www.deswater.com
doi: 10.1080/19443994.2015.1091987

57 (2016) 18300–18313
August

Taylor & Francis
Taylor & Francis Group

Adsorption of PAEs from aqueous solution by modified zeolites

Yufeng Xu[a], Long Wang[b], Simin Li[a,*], Wei Zhang[a], Qiang Jing[a], Jinghan Cao[a]

[a]*College of Urban Construction, Hebei University of Engineering, Handan 056038, China, Tel. +86 310 857 8756; emails: jackstarfly@126.com (Y. Xu), chyeli@126.com (S. Li), 354477493@qq.com (W. Zhang), 535428459@qq.com (Q. Jing), 609159925@qq.com (J. Cao)*

[b]*Chongqing Academy of Metrology and Quality Inspection, Chongqing 401123, China, Tel. +86 21 6751 5903; email: cquwang@163.com*

Received 14 January 2015; Accepted 26 August 2015

ABSTRACT

Natural zeolites (NZ), zeolites modified with hexadecyl trimethylammonium bromide (CTMZ), and zeolites modified with hexadecyl trimethyl ammonium bromide/sodium dodecyl sulfate (CSMZ) were prepared and used for the adsorption of phthalate esters (PAEs). The adsorbents were characterized using scanning election microscopy, X-ray diffraction, Fourier transform infrared spectroscopy, and thermogravimetric, Brunauer–Emmett–Teller, and organic carbon analyses. Adsorption characteristics, such as kinetics, isotherms, thermodynamics, and renewability, were also evaluated. The amount of PAEs adsorbed followed the order of CSMZ > CTMZ > NZ at all adsorption times. The kinetic data were fitted into three kinetic models, namely, pseudo-first-order, pseudo-second-order, and intra-particle diffusion. The pseudo-second-order model was the most suitable in describing the experimental process. The adsorption isotherms were also correlated using four different models. The equilibrium adsorption data of PAEs fitted better with the linear isotherm model for CTMZ and CSMZ and with the non-linear isotherm model for NZ. Hence, partition primarily contributes to PAEs adsorption onto CTMZ and CSMZ. PAEs adsorption onto NZ, CTMZ, and CSMZ was spontaneous and exothermic in nature, and was not affected by pH. The regeneration experiment results showed that CTMZ and CSMZ are potential adsorbents because of their low cost and reusability.

Keywords: Zeolites; Adsorb; PAEs; Kinetics; Isotherms; Thermodynamics; Renewable

1. Introduction

Environmental pollution by phthalate esters (PAEs) is an important issue in worldwide environmental chemistry. PAEs affect endocrine, respiratory, and reproductive functions and cause developmental toxicity [1]. PAEs are synthetic compounds added as plasticizer to improve the flexibility, transparency, durability, and longevity of plastics in the cosmetic, ceramic, paper, and paint industries [2]. As PAEs exist in a freely mobile and leachable phase, instead of being chemically bound to the matrix of plastic or other products, they can evaporate, leach, or migrate into the environment. PAEs have been detected within the range of ng/L–mg/L in the effluents of wastewater treatment plants, surface water bodies, and drinking water. PAEs concentrations in wastewater from chemical plants or nearby rivers and plasticizer factories

*Corresponding author.

have reached 100 mg/L [3]. PAEs have been classified as a priority pollutant and an endocrine-disrupting compound by the European Environment Agency and US Environmental Protection Agency because of its large production and extensive distribution [4].

PAEs can be biodegraded or mineralized, with half-lives ranging from 1 d to several months, depending on the length and structure of side chains [5,6]. PAEs are difficult to remove from aquatic media, and only a part can be recovered through typical wastewater treatment systems. Researchers also believe that PAEs cannot be eliminated from sewage through municipal wastewater treatment facilities. Al-Odaini et al. [7–9] employed various processes, including ultrafiltration [10–13], nanofiltration [14], reverse osmosis [15,16], and adsorption [16], to effectively remove PAEs from aqueous media. Of these processes, adsorption can effectively remove organic matter from waste effluents. As a popular adsorbent, activated carbon is used to remove contaminants from water [17,18], but is associated with high cost and regeneration difficulty [19]. Zeolites are applied as an alternative adsorbent to activated carbon because of their renewability, low cost, local availability, and effectiveness [20]. Natural zeolites (NZ) are highly porous hydrated alumina silicate materials with a framework formed by tetrahedra of SiO_4 and AlO_4, and contain water molecules, alkali, and alkaline earth metals [21]. As a natural adsorbent with a porous structure, zeolites exhibit high ion-exchange capacity and specific surface areas. Given that some organic compounds exhibit limited adsorption capacity on zeolites, several studies have modified zeolites by using cationic surfactants. The exchangeable cations on the external surface of zeolite are readily exchanged with the positive head groups of the cationic surfactants to form surfactant monolayers. Under suitable conditions, the anionic–cationic surfactants form bilayers on the external surface of zeolite, in which the upper layer is bound to the lower layer through hydrophobic interaction.

This investigation evaluated contact time, temperature, and solution pH to determine the possible environmental factors that affect the interaction between PAEs and adsorbents. The following adsorbents were prepared: NZ; zeolites modified with hexadecyl trimethyl ammonium bromide (CTMAB), named CTMZ; and zeolites modified with CTMAB/sodium dodecyl sulfate (SDS), named CSMZ. Experimental results were analyzed with kinetic and isotherm models. This research would provide useful information about PAEs removal through adsorption to decrease the exposure concentration of PAEs in the environment.

NZ, CTMZ, and CSMZ were prepared and used as adsorbents to remove PAEs from aqueous solution. These adsorbents were characterized using X-ray diffraction (XRD), organic carbon analysis, thermogravimetric analysis (TGA), Fourier transform infrared (FT-IR) spectroscopy, Brunauer–Emmett–Teller (BET) analysis, and scanning election microscopy (SEM). PAEs adsorption efficiencies were compared among NZ, CTMZ, and CSMZ. The effects of experimental parameters, namely, contact time, temperature, and solution pH, were also investigated. Experimental results were analyzed using kinetic and isotherm models, and thermodynamic parameters, such as changes in Gibbs free energy, enthalpy, and entropy were calculated. The reproducibility of NZ, CTMZ, and CSMZ was further evaluated.

2. Experimental

2.1. Materials

NZ was obtained from a mineral deposit in Jinyun County, Zhejiang Province, China. NZ was crushed and sieved to obtain a particle size smaller than 0.075 mm. The chemical composition of NZ is as follows (in mass): 69.48% SiO_2, 12.0% Al_2O_3, 0.87% Fe_2O_3, 1.33% K_2O, 0.23% MgO, 2.59% CaO, 2.59% Na_2O, and 10.91% others.

Two representative types of PAEs, namely, dimethyl phthalate (DMP) and bis (2-ethylhexyl) phthalate (DEHP), were selected based on polarity and molecular size. DMP and DHEP were purchased from National Standard Substance Center, with log-K_{ow} values of 1.6 and 7.6, respectively, and molecular sizes of 194 and 390, respectively. CTMAB and SDS were of analytical reagent grade and purchased from Sinopharm Chemical Reagent Co Ltd, China.

2.2. Preparation of CTMZ and CSMZ

CTMZ was prepared by mixing 20.0 g of NZ and 1.0 g of CTMAB in 100 mL of Milli-Q water on a shaker equipped with a thermostat at 30˚C for 2 h. The mixture was centrifuged, and the supernatants were discarded. The precipitate was rinsed using Milli-Q water several times (until the surfactant cannot be detected), heated at 100˚C, and then placed in a dryer.

CSMZ was prepared by mixing 20.0 g of NZ, 0.655 g of CTMAB, and 0.345 g of SDS in 100 mL of Milli-Q water on a shaker equipped with a thermostat at 30˚C for 2 h. The mixture was centrifuged, and the

supernatants were discarded. The precipitate was rinsed using Milli-Q water several times (until surfactants cannot be detected), heated at 100℃, and then placed in a dryer.

2.3. Characterization

Organic carbon was analyzed in the three absorbents through potassium dichromate oxidation and titration with ferrous sulfate. FT-IR spectra of the samples were obtained using an FT-IR spectrometer (Nicolet AVATAR 370, Thermo Nicolet Co., USA). XRD patterns were obtained using an X-ray diffractometer (Rigaku D/MAX2200PC Rigaku Inc., Japan). TGA curves of solid samples were conducted using a TGA (DSC 141, SETARAM Inc., France) and heated from 50 to 600℃. BET analysis was performed using an advanced Nova system (ASAP 2010, Micromeritics Inc., USA) with liquid N_2 at 196℃. SEM analysis was performed using a scanner (VEGA II, TESCAN Inc., Czechia).

2.4. Adsorption experiments

PAEs (DMP and DHEP) were removed from the solutions through adsorption using NZ, CTMZ, or CSMZ in a batch system. Adsorption experiments were conducted using different adsorbent amounts, temperatures, and initial solution pH. For all batch experiments, the mixture of PAEs solution and adsorbent was placed on a shaker equipped with a thermostat at 180 rpm and at a specified temperature for 24 h. The desired pH of the solution was maintained by adding 0.1 mol/L HCl or NaOH. Residual PAEs concentration was determined by high-performance liquid chromatography (SHIMADZU LC-20A, Shimadzu, Japan). Isotherm studies were conducted by varying the temperature from 10 to 35℃. The equilibrium of adsorption was evaluated with the following isotherm models: linear, Langmuir, Freundlich, and adsorption–partitioning model. All experiments were performed in duplicate.

2.5. Regeneration of saturated zeolites

Reuse and recovery of spent adsorbents are important in wastewater treatment. Regeneration experiments were designed using the desorption behavior to regenerate saturated adsorbents in NaCl solution under neutral pH for 3 h. The zeolites were then washed with Milli-Q water and used repeatedly after being dried.

3. Results and discussion

3.1. Properties of natural and modified zeolites

Table 1 shows the surface area and average pore diameter distributions (inset) of NZ, CTMZ, and CSMZ. The International Union of Pure and Applied Chemistry classifies pores based on diameter (d) into three categories: micropores ($d < 2$ nm), mesopores (2 nm $< d <$ 50 nm), and macropores ($d > 50$ nm). Based on this classification, the pore diameter distribution of NZ, CTMZ, and CSMZ was mesoporous, which is similar to the findings of Lin and Zhan [22], who characterized surfactant-modified zeolites. The surface areas and pore diameter of the zeolites decreased when modified with the cationic surfactants CTMAB and SDS. This phenomenon could be due to the obstruction of the main pore channels of CTMZ and CSMZ by surfactant molecules, thereby impeding the diffusion of N_2 throughout the channels [23].

The results of organic carbon analysis of various absorbents showed that CTMZ and CSMZ contain organic carbon (Table 2).

The morphology of the samples is shown in Fig. 1. The images showed that the surface morphology differed among NZ, CTMZ, and CSMZ. NZ was characterized by aggregated morphology, massiveness, and large flakes. After modification, the surface of CTMZ and CSMZ showed white flakes with severely crumpled structures. The morphological changes in the samples were attributed to the coverage of the surfactant on CTMZ and CSMZ, thus confirming the combination of NZ and the surfactant.

The XRD patterns of NZ, CTMZ, and CSMZ are shown in Fig. 2. The five main peaks in the 2θ region

Table 1
BET of NZ, CTMZ, and CSMZ

	Average pore size(nm)	Surface area (m^2/g)
NZ	22.43	41.5
CTMZ	18.18	24.1
CSMZ	11.03	20.0

Table 2
Organic carbon contents of NZ, CTMZ, and CSMZ

	Organic carbon (%)	Multiple
NZ	0.136	1
CTMZ	0.370	2.7
CSMZ	0.955	7.0

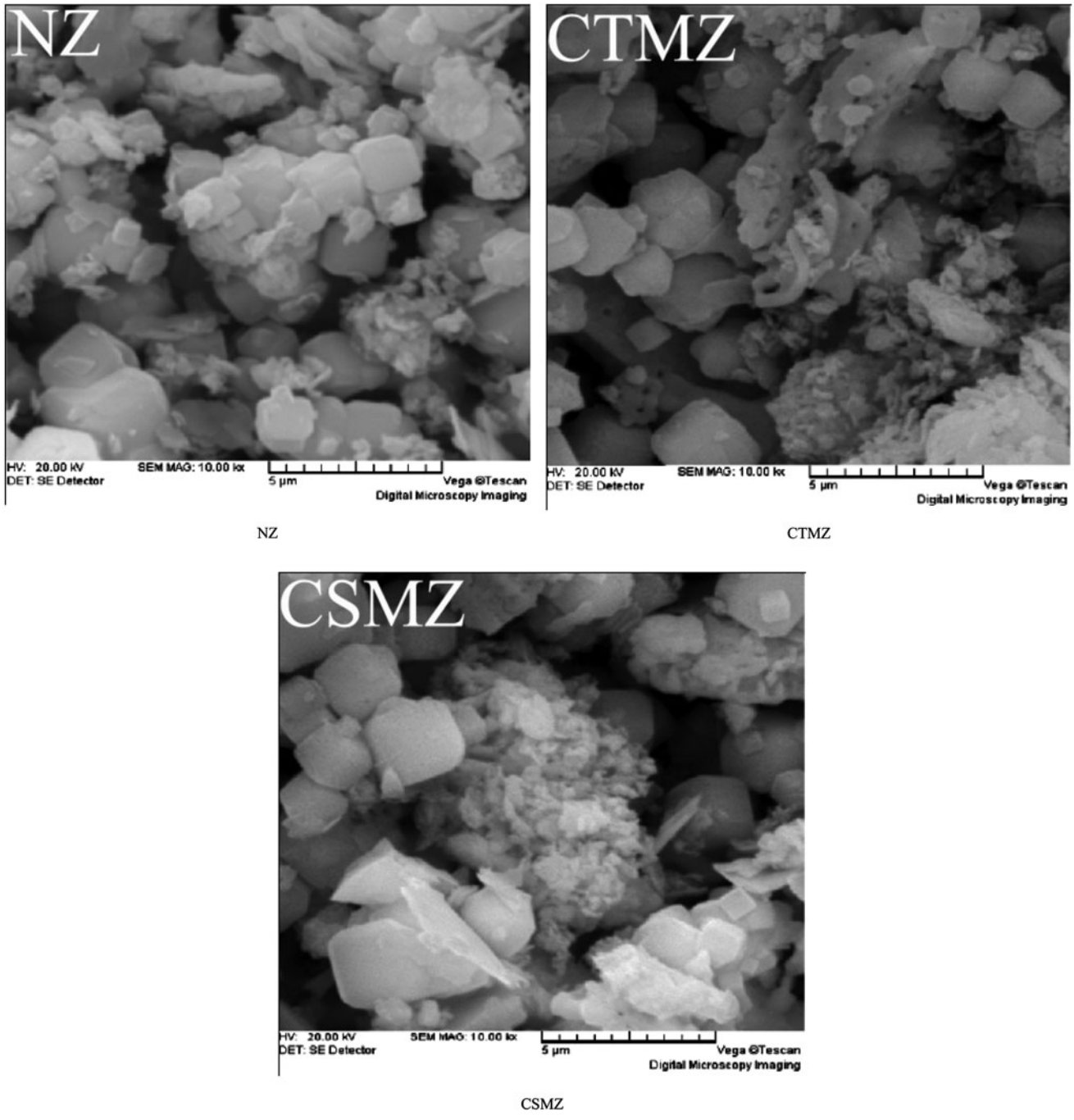

Fig. 1. SEM images of NZ, CTMZ, and CSMZ.

(9.828˚, 22.392˚, 26.440˚, 26.640˚, and 28.016˚) are the characteristic of mordenite according to the Joint Committee on Powder Diffraction Standard (JCPDS) data. The main peaks correspond to SiO_2 and Al_2O_3 (JCPDS 89-1666 and 88-0826). The low relative intensities of the peaks at 2θ (18˚, 19˚, and 21˚) in CTMZ and CSMZ were the consequence of surface modification by the surfactant and correspond to Br, thereby confirming that CTMAB was incorporated into the zeolite. In conclusion, the diffraction peaks of NZ, CTMZ, and CSMZ are similar, which indicates that their internal structure is uniform.

The FTIR spectra of NZ, CTMZ and CSMZ are shown in Fig. 3. The FTIR spectra of NZ showed

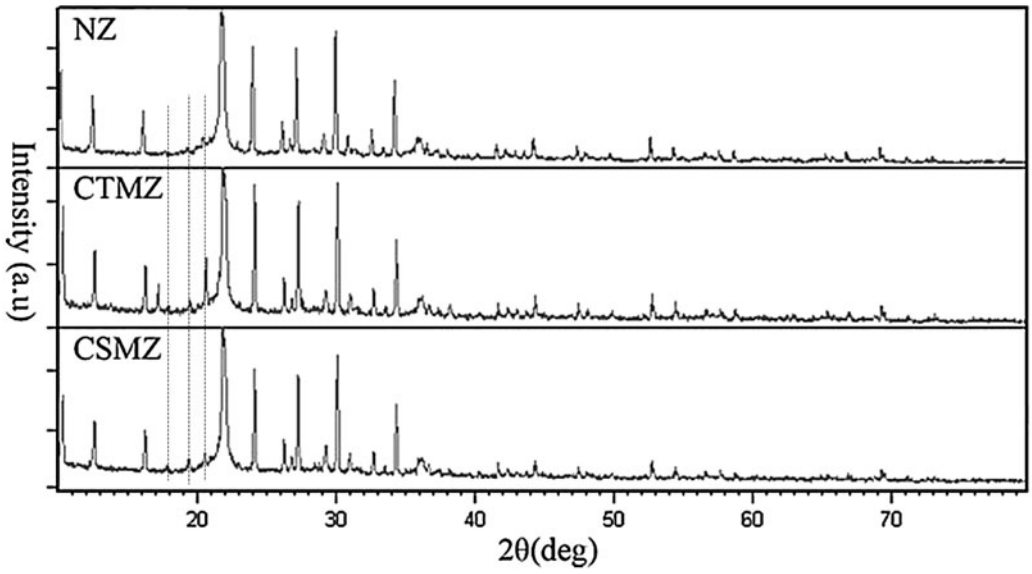

Fig. 2. XRD spectra of NZ, CTMZ, and CSMZ.

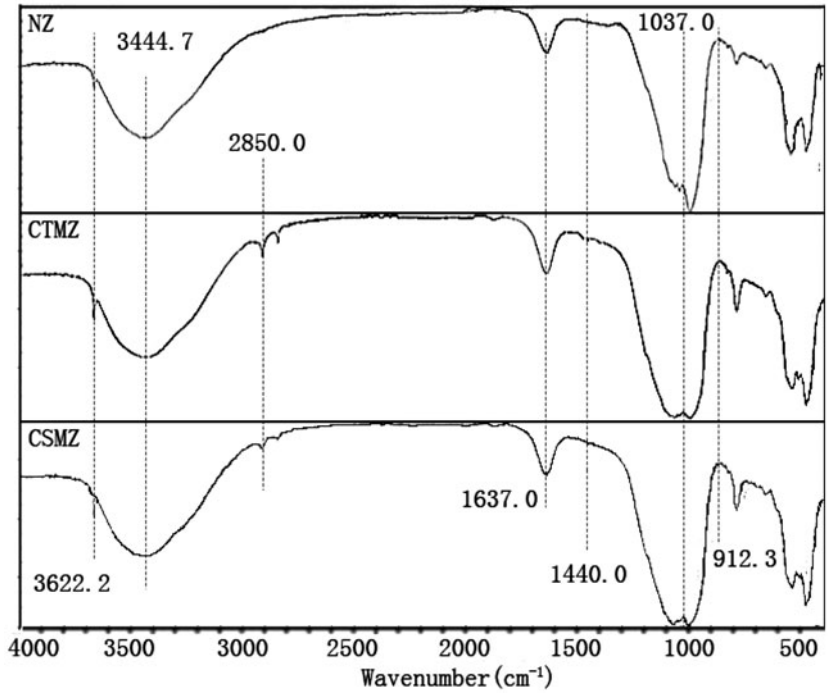

Fig. 3. IR spectra of NZ, CTMZ, and CSMZ.

similar characteristics to that reported by Elaiopoulos et al. [24]. Compared with pure NZ, the new specific bands in the FTIR spectra of CTMZ and CSMZ at 2,800–2,900 and 1,400–1470 cm^{-1} correspond to the stretching and deformation vibrations in the $-CH_2$ groups of CTMAB. This finding confirmed that the cationic surfactant was adsorbed onto the NZ surface through surface modification. Meanwhile, the bands in the FTIR spectra of CSMZ within the range of 2,850–2,921 and 1,219–1,259 cm^{-1}, which correspond to the aliphatic and the sulfate groups of SDS, respectively, was not obvious because of the aggregation

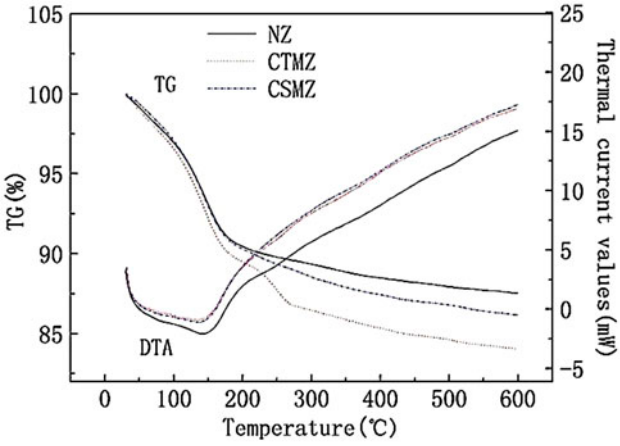

Fig. 4. TG and DTA curves of NZ, CTMZ, and CSMZ.

behaviors of the anionic–cationic surfactant composite [25].

The differences in the relative intensities in the XRD patterns and FTIR spectra between CTMZ and CSMZ could be due to the admixture of CTMAB and SDS.

The thermal stability of NZ, CTMZ, and CSMZ at increased temperatures was determined through TGA [26]. The TGA curves of NZ, CTMZ, and CSMZ, which presented several mass loss steps, are shown in Fig. 4. The mass loss at temperatures lower than 200℃ is attributed to the unbound and physically adsorbed water [23], whereas the mass loss between 200 and 600℃ is attributed to the decomposition of organic molecules. The weight loss was similar among NZ, CTMZ, and CSMZ at temperatures lower than 193℃ but significantly differed between 200 and 600℃. The weight loss of NZ at temperatures between 190 and 600℃ is mainly attributed to the decomposition of organic molecules, and the total weight loss was approximately 3.5%. The weight loss of CTMZ at temperatures between 190 and 600℃ is mainly attributed to the decomposition of CTMAB, and the total weight loss was found to be about 6%. The weight loss of CSMZ at temperatures between 190 and 600℃ is mainly attributed to the decomposition of CTMAB and SDS, and the total weight loss was approximately 4.5%. The weight loss between 200 and 600℃ was higher in CTMZ and CSMZ than that in NZ, thus confirming that the cationic surfactant entered into the pores of the zeolite, or was adsorbed on the surface through surface modification. The weight loss between 200 and 600℃ was also higher in CTMZ than that in CSMZ, which indicated that the anionic–cationic modification differs from simple cationic modification.

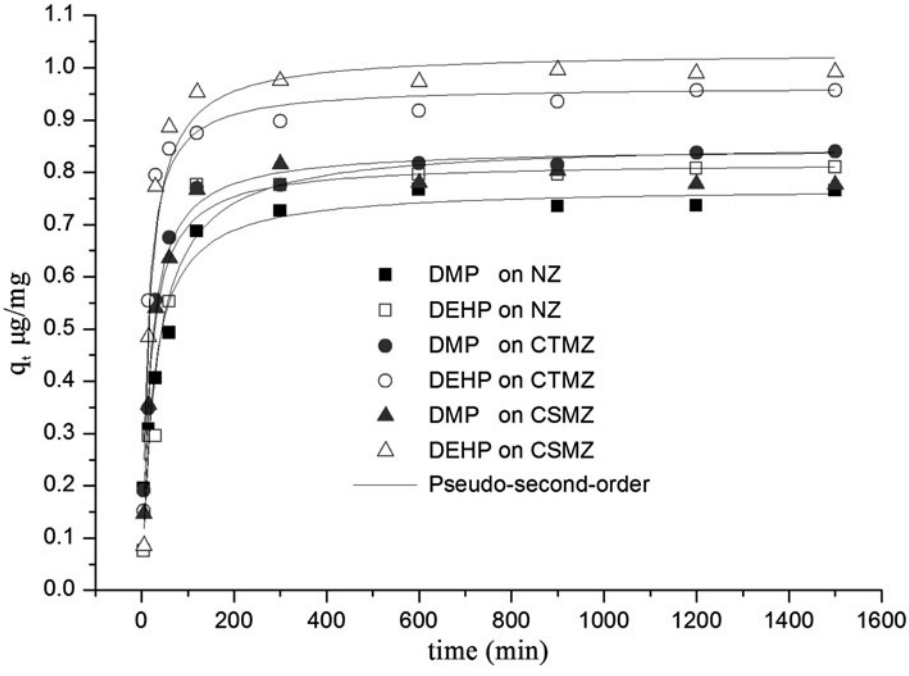

Fig. 5. Effect of agitation time on adsorption of PAEs on NZ, CTMZ, and CSMZ.

3.2. Adsorption kinetics

Adsorption experiments of PAEs were performed at 30°C under a pH of 6.36 for up to 20 h. The kinetics of PAEs adsorption onto NZ, CTMZ, and CSMZ are shown in Fig. 5 and Table 3. The kinetics of PAEs adsorption presented a two-step process. PAEs adsorption mostly occurred within 40 min of contact time. The rapid adsorption in the first stage was due to the availability of the cationic-charged surface of the adsorbent and the effect of surface absorption. The second stage was attributed to the slow adsorption period; the remaining vacant surface sites were difficult to occupy because of the repulsive forces between adsorbate molecules in the aqueous solution and those on the adsorbent surface [27]. The adsorption kinetics almost reached equilibrium within 150 min. The adsorption rate of DEHP was higher than that of DMP. Liu et al. [1] reported that adsorption rate was closely related to the straight carbon chain length and followed the order of DMP < DEP < DiBP < DBP < DEHP. From Table 1, we can presume that the surface area and average pore diameter distributions of the adsorbents did not remarkably affect adsorption. NZ, which has high sur-

Table 3
Fitting of the kinetic parameters of PAEs adsorption on NZ, CTMZ, and CSMZ

		Pseudo-first-order model			Pseudo-second-order model			Intra-particle diffusion model		
		q_e	k_1	R^2	q_2	k_2	R^2	K_{id}	C_i	R^2
DMP	NZ	0.729	0.027	0.923	0.769	0.055	0.965	0.015	0.333	0.6555
	CTMZ	0.807	0.038	0.979	0.851	0.068	0.981	0.015	0.419	0.5302
	CSMZ	0.784	0.037	0.981	0.828	0.067	0.984	0.015	0.405	0.4906
DEHP	NZ	0.809	0.024	0.884	0.867	0.037	0.942	0.019	0.305	0.4740
	CTMZ	0.924	0.058	0.914	0.971	0.090	0.974	0.014	0.561	0.3328
	CSMZ	0.992	0.019	0.959	1.067	0.025	0.990	0.024	0.332	0.6030

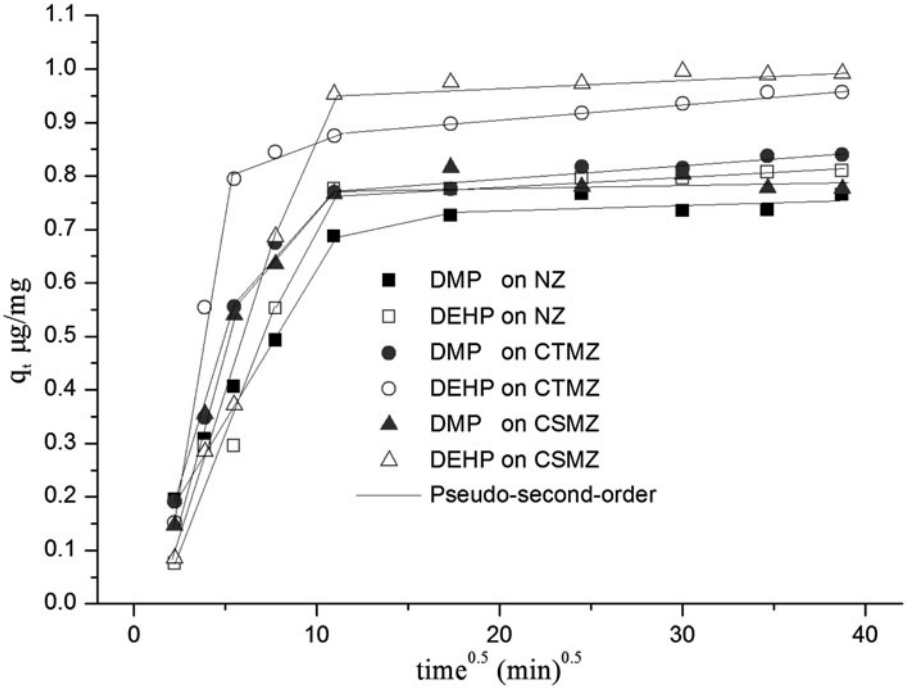

Fig. 6. Intra-particle diffusion plots for adsorption of PAEs on NZ, CTMZ, and CSMZ.

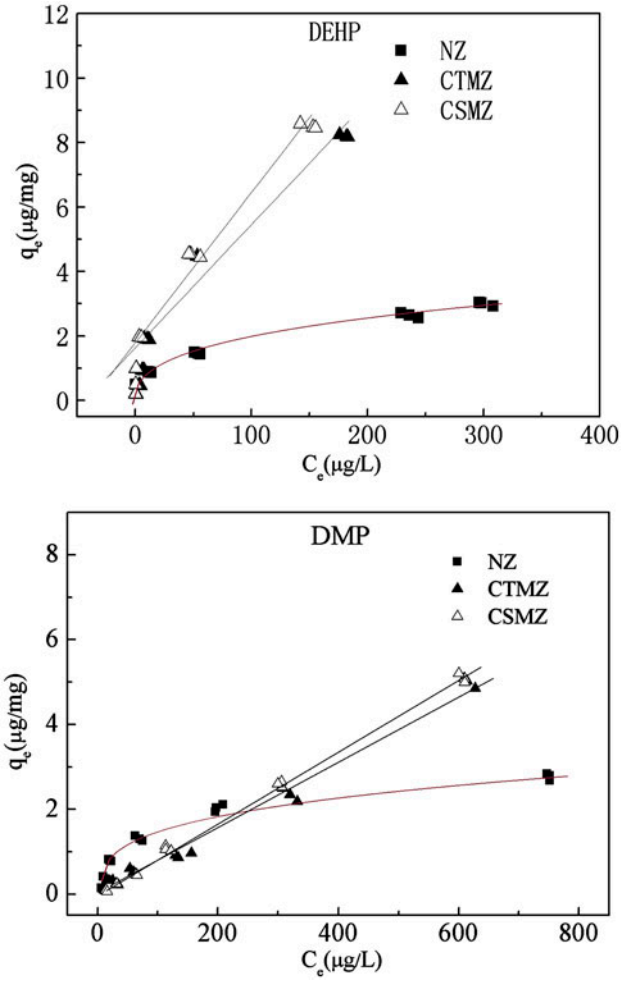

Fig. 7. Adsorption isotherm plots of PAEs on NZ, CTMZ, and CSMZ.

face area and pore diameter, exhibited a lower adsorption rate than CTMZ and CSMZ, which present low surface area and pore diameter.

The kinetic parameters of PAEs adsorption onto NZ, CTMZ, and CSMZ are shown in Table 3. The kinetic rates of PAEs followed the pseudo-second-order model for the entire adsorption period, with an R^2 value of 0.94–0.98. Hence, we can infer that the rate-limiting step is the chemisorption stage.

The plots of q_t vs. $t^{0.5}$ for the adsorption of PAEs onto NZ, CTMZ, and CSMZ are shown in Fig. 6. The adsorption process was controlled by three different stages: (1) rapid external surface adsorption, (2) diffusion into the adsorbent particles through the interlayer space, and (3) final equilibrium stage [28]. These stages indicate that the external mass transfer (boundary layer diffusion) and intra-particle diffusion simultaneously occur during the gradual adsorption stage.

3.3. Adsorption isotherms

The adsorption isotherms of PAEs onto NZ, CTMZ, and CSMZ at pH 6.36 and 30˚C are shown in Fig. 7. The adsorption capacities for PAEs increased with increasing PAEs concentration until equilibrium was reached. The adsorption capacity for the same PAEs followed the order of CSMZ > CTMZ > NZ. The amount of PAEs adsorbed on CSMZ was higher than that on CTMZ, and the amounts adsorbed on both CSMZ and CTMZ were higher than those on NZ at all adsorption times. Thus, CTMZ and CSMZ are promising adsorbents for removing PAEs.

Linear, Langmuir, Freundlich, and adsorption–partitioning models were used to describe the experimental results and elucidate the adsorption mechanism. The linear isotherm model describes adsorbate partition in a solution and the adsorbent surface to evaluate the sorption behavior [29,30]. The Freundlich isotherm model describes the non-ideal

Table 4
Linear, Langmuir, Freundlich, and adsorption-partition isotherms of PAEs on NZ, CTMZ, and CSMZ

	Eq.	Langmuir $\frac{C_e}{q_e}=\frac{1}{K_L Q_M}+\frac{C_e}{Q_M}$			Freundlich $q_e = K_F \cdot C_e^{\frac{1}{n}}$			Linear $q_e = K_L \cdot C_e + b$			Adsorption-partition $q_e = K_{if} C_e^n + K_p C_e$			
		R^2	K_L	Q_M	R^2	K_F	n	R^2	K_L	b	R^2	K_{if}	K_p	n
DMP	NZ	0.93	0.01	3.32	0.80	0.28	2.65	0.57	0.003	0.75	0.98	0.170	−0.118	0.949
	CTMZ	0.99	0.001	11.7	0.98	0.048	1.42	0.95	0.008	−0.03	0.99	−0.145	0.148	0.995
	CSMZ	0.99	0.001	12.36	0.98	0.06	1.45	0.99	0.01	−0.12	0.99	0.181	−0.172	0.999
DEHP	NZ	0.97	0.018	3.40	0.87	0.368	2.28	0.69	0.008	0.603	0.99	0.469	0.0036	0.246
	CTMZ	0.98	0.013	11.5	0.99	0.44	1.77	0.97	0.041	1.09	0.99	0.560	−0.306	0.910
	CSMZ	0.96	0.013	12.7	0.99	0.83	2.21	0.96	0.047	1.66	0.99	1.186	0.029	0.248

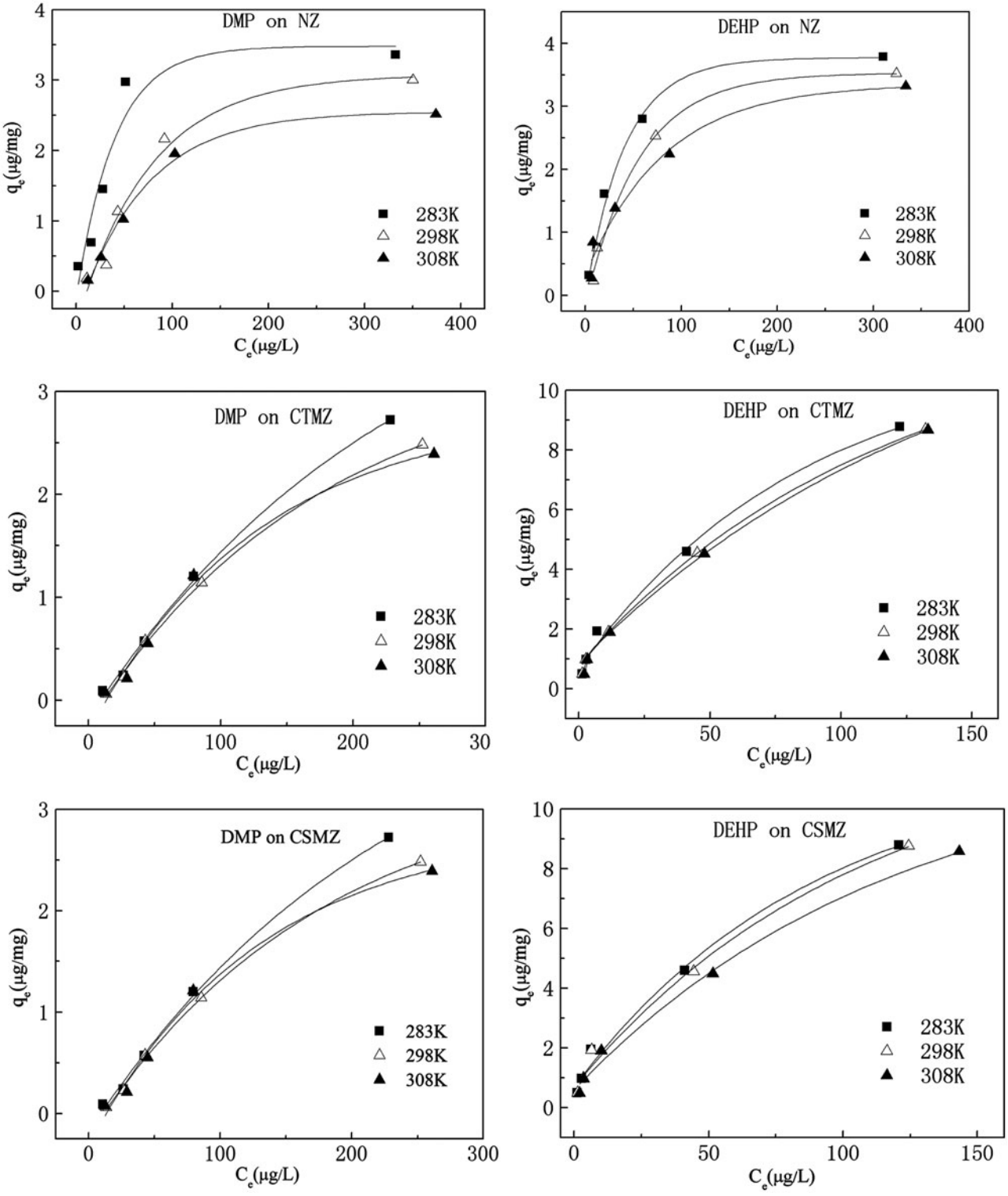

Fig. 8. Effect of temperature on PAEs adsorption on NZ, CTMZ, and CSMZ.

adsorption of a heterogeneous system and reversible adsorption [31]. The Langmuir isotherm model assumes that the forces of interaction between the adsorbate molecules are negligible, after adsorbate molecules occupy the adsorption site, they cease to perform further adsorption [32]. The

adsorption–partitioning model is the combination of the linear and Freundlich isotherm models [33,34].

Table 4 shows the parameters of the linear, Langmuir, Freundlich, and adsorption–partition models. The isothermal curves significantly differed among PAEs adsorption onto NZ, CTMZ, and CSMZ. The best-fitted adsorption isotherm models of PAEs adsorbed on NZ were found to be Langmuir > adsorption–partition > Freundlich > linear, whereas those on CTMZ and CSMZ were found to be: adsorption–partition > Langmuir > Freundlich > linear. The results showed a better fit to the linear equation for CTMZ with R^2 = 0.95–0.97, and CSMZ with R^2 = 0.96–0.99 than NZ with R^2 = 0.57–0.69. Hence, organic partition primarily contributes to PAEs adsorption onto CTMZ and CSMZ.

As NZ contains net negative structural charges in their frameworks and PAEs are nonpolar substances, NZ presents low adsorption capacity for PAEs because of the surface absorption mechanism. The high adsorption efficiency of PAEs onto CTMZ and CSMZ is attributed to the CTMAB and CTMAB/SDS layers. After modification, the hydrophobic interaction of the CTMZ and CSMZ surfaces increased and PAEs adsorption onto CTMZ and CSMZ was due to hydrophobic interaction. However, DEHP with high octanol–water partition coefficient showed a high removal rate. Thus, we can conclude that the adsorption capacity of PAEs on CTMZ and CSMZ is higher than that on NZ because of (1) the hydrophobic interaction between the hydrophobic tails of the CTMAB and CTMAB/SDS layers and the hydrophobic functional groups of PAEs molecules; and (2) the partitioning of PAEs molecules into the CTMAB and CTMAB/SDS layers.

3.4. Effect of temperature

The equilibrium of PAEs adsorption onto NZ, CTMZ, and CSMZ was investigated at three different temperatures (283, 298, and 308 K) under a solution pH of 6.36 (Fig. 8). Thermodynamic parameters, including changes in Gibbs free energy (G), enthalpy (H), and entropy (S), were calculated using the following equations to determine the mechanism underlying the adsorption process:

$$\Delta G = -RT \ln K_L \quad (1)$$

$$\Delta G = \Delta H - T\Delta S \quad (2)$$

where K_L is the distribution coefficient (L/mol), R is the universal gas constant (8.314 J/mol K), and T is the temperature (Kelvin, K). The calculation results are listed in Table 5. G represents the feasibility of spontaneous and exothermic nature in the adsorption process of PAEs on NZ, CTMZ, and CSMZ. In general, the G value ranges from −20 to 0 kJ/mol for physisorption, and −400 and −80 kJ/mol for chemisorption [35]. In this study, the values of G were under the range for physisorption, thereby confirming that the mechanisms of PAEs adsorption onto NZ, CTMZ, and CSMZ at a solution pH of 6.36 does not include anion exchange and electrostatic attraction. The negative value of H indicates that the adsorption process is exothermic in nature. The energy of adsorption from different forces is classified as follows: Van der Waals forces, 4–10 kJ/mol; hydrophobic bond forces, 5 kJ/mol; hydrogen bond forces, 2–40 kJ/mol; coordination exchange, 40 kJ/mol; dipole bond forces, 2–29 kJ/mol; and chemical bond forces, >60 kJ/mol [36]. In this study, the value of H was 12–15 kJ/mol in PAEs adsorption onto NZ, which indicated that dipole bond forces are important in the adsorption process. Meanwhile, the value of H was 2–6 kJ/mol in PAEs adsorption onto CTMZ and CSMZ, which implied that Van der Waals forces and hydrophobic bond forces are important in the adsorption process.

Table 5
Thermodynamic parameters, ΔH°, ΔS°, and ΔG°, for PAEs adsorption on NZ, CTMZ, and CSMZ at 283, 298, ands 308 K

		NZ			CTMZ			CSMZ		
	K	ΔG (kJ/mol)	ΔS (J/mol K)	ΔH (kJ/mol)	ΔG (kJ/mol)	ΔS (J/mol K)	ΔH (kJ/mol)	ΔG (kJ/mol)	ΔS (J/mol K)	ΔH (kJ/mol)
DMP	283	−3.82	−30.8	−12.4	−2.71	−6	−4.39	−2.03	3.49	−2.1
	298	−2.89			−2.54			−1.99		
	308	−3.15			−2.57			−2.04		
DEHP	283	−4.14	−39	−15.2	−4.1	4.82	−5.62	−3.93	2.79	−3.2
	298	−3.67			−4.12			−4.02		
	308	−3.15			−3.95			−3.99		

3.5. Effect of pH

The pH of aqueous solution is an important variable that governs the adsorption of PAEs and can be manipulated to control the adsorption process and capacity. The adsorption curves of PAEs on NZ, CTMZ, and CSMZ at four different pH values are illustrated in Fig. 9. The DEHP adsorption capacity was slightly influenced by solution pH at 5.0–9.0,

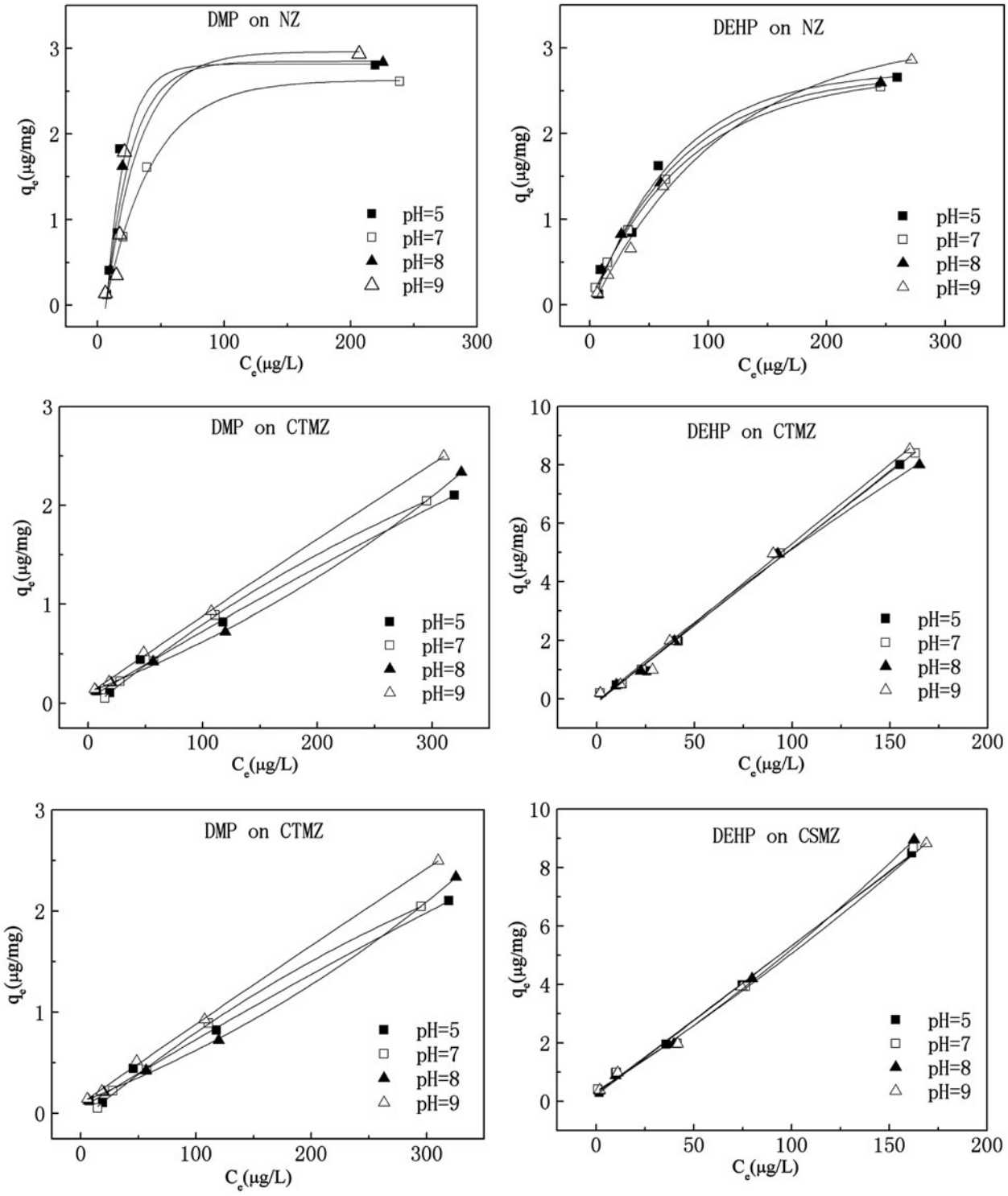

Fig. 9. Relationship between pH and the adsorption efficiency of PAEs on NZ, CTMZ, and CSMZ.

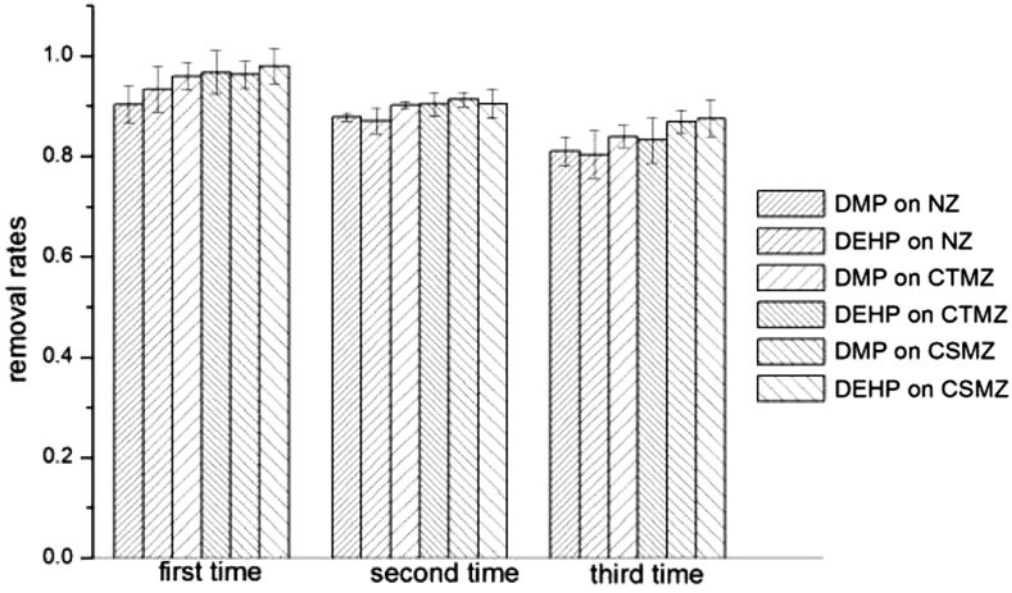

Fig. 10. Comparison of the removal performance of PAEs on original and regenerative adsorbents.

which indicated that the adsorption of DEHP on the positively charged surface of adsorbent is unlikely to be driven by electrostatic attraction, but by organic partitioning. The adsorption of DMP on the adsorbent increased with increasing pH. As DMP stability is correlated with solution pH, the remaining DMP in the solution decreased with increasing pH because DMP is decomposed in high pH solution.

3.6. Regeneration performance of adsorbents

Regeneration is performed to remove residual PAEs from the zeolite adsorbents. Regeneration not only removes zeolite water and organic matters, but also maintains the structure of the zeolite adsorbents. The two main regeneration methods include (1) using lime as the regeneration agent in high pH regeneration and (2) using NaCl as the regeneration agent in neutral pH regeneration. Based on the cost, risk, and effect on the environment, NaCl was used for regeneration of the adsorbent in this study.

Regenerative adsorbents were reloaded with PAEs solution of selected concentrations to check the regeneration performance of NZ, CTMZ, and CSMZ. Fig. 10 shows the removal performance of PAEs using original and regenerative adsorbents with the same initial pH value, temperature, and adsorbent dosage. The gradual reduction in the adsorption capacity of adsorbents was observed during regeneration processes. The average adsorption capacity reduced in steps from 92 to 80%, 95 to 82%, and 96 to 85% for NZ, CTMZ, and CSMZ, respectively. The reduced adsorption performance may be due to the partial destruction of the structure of the adsorbents during regeneration.

The adsorbents were regenerated using NaCl through three parts: (1) the desorption of adsorbent in NaCl solution and recovery of the adsorption capacity of adsorbent, (2) Na ion replacement for Mg and Ca to increase the zeolite surface adsorption sites, and (3) modification of the surface morphology of the zeolite with NaCl [37]. As surface adsorption and organic partitioning are responsible for the adsorption of PAEs in this study, desorption is the main controlling factor during regeneration. The adsorption capacity of the adsorbent decreased with increasing amount of PAEs residues.

Overall, this study showed that the removal performance of PAEs was similar when using original and regenerative adsorbents. Hence, these adsorbents are suitable for repeated use and are considered as ideal renewable adsorbent for PAEs adsorption.

4. Conclusions

The amounts of PAEs adsorbed followed the order of CSMZ > CTMZ > NZ at all adsorption times. This study showed that CTMZ and CSMZ can be used as low-cost and reusable adsorbent for the removal of PAEs from water. The adsorption kinetics of PAEs on NZ, CTMZ, and CSMZ obeyed a pseudo-second-order model. The intra-particle diffusion model indicated that adsorption occurred in three distinct stages. The

equilibrium adsorption data of PAEs on CTMZ and CSMZ fitted better with the linear isotherm model, whereas NZ fitted better with the non-linear isotherm model. This finding implied that organic partitioning is responsible for the adsorption of PAEs onto CTMZ and CSMZ. Assessment of thermodynamic parameters indicated that the adsorption of PAEs onto NZ, CTMZ, and CSMZ was spontaneous and exothermic. Meanwhile, the effect of pH on the adsorption of PAEs onto NZ, CTMZ, and CSMZ could be neglected. Dipole bond forces are important in the adsorption process of PAEs on NZ, whereas Van der Waals forces and hydrophobic bond forces are important on CTMZ and CSMZ. The results of regeneration study showed that the removal performance of PAEs was similar when using original and regenerative adsorbents. The average adsorption capacity decreased in steps from 92 to 80%, 95 to 82%, and 96 to 85% for NZ, CTMZ, and CSMZ, respectively. This work demonstrates that CTMZ and CSMZ are ideal renewable adsorbents for PAEs adsorption.

Acknowledgment

This work was supported by the Major Science and Technology Program for Water Pollution Control and Treatment (No. 2012ZX07203-003), Major Basic Research Program of Hebei Foundation Research (No. 12966738D), Natural Science Foundation of Hebei Province (No. E2014402101) and Handan Science and Technology Research Program (1213109010G).

References

[1] H. Liu, D. Zhang, M. Li, L. Tong, L. Feng, Competitive adsorption and transport of phthalate esters in the clay layer of JiangHan plain, China, Chemosphere 92 (2013) 1542–1549.
[2] G. Wen, J. Ma, Z. Liu, L. Zhao, Ozonation kinetics for the degradation of phthalate esters in water and the reduction of toxicity in the process of O3/H2O2, J. Hazard. Mater. 195 (2011) 371–377.
[3] G. Mailhot, M. Sarakha, B. Lavedrine, J. Cáceres, S. Malato, Fe(III)-solar light induced degradation of diethyl phthalate (DEP) in aqueous solutions, Chemosphere 49 (2002) 525–532.
[4] Z.P. Lin, M.G. Ikonomou, H. Jing, Determination of phthalate ester congeners and mixtures by LC/ESI-MS in sediments and biota of an urbanized marine inlet, Environ. Sci. Technol. 37 (2003) 2100–2108.
[5] W. Jianlong, L. Ping, S. Hanchang, Q. Yi, Biodegradation of phthalic acid ester in soil by indigenous and introduced microorganisms, Chemosphere 35 (1997) 1747–1754.
[6] S. Amir, M. Hafidi, G. Merlina, H. Hamdi, A. Jouraiphy, M. El Gharous, J.C. Revel, Fate of phthalic acid esters during composting of both lagooning and activated sludges, Process Biochem. 40 (2005) 2183–2190.
[7] N.A. Al-Odaini, M.P. Zakaria, M.I. Yaziz, S. Surif, Multi-residue analytical method for human pharmaceuticals and synthetic hormones in river water and sewage effluents by solid-phase extraction and liquid chromatography–tandem mass spectrometry, J. Chromatogr. A 1217 (2010) 6791–6806.
[8] R. Loos, B.M. Gawlik, G. Locoro, E. Rimaviciute, S. Contini, G. Bidoglio, EU-wide survey of polar organic persistent pollutants in European river waters, Environ. Pollut. 157 (2009) 561–568.
[9] K. Luks-Betlej, P. Popp, B. Janoszka, H. Paschke, Solid-phase microextraction of phthalates from water, J. Chromatogr. A 938 (2001) 93–101.
[10] Y. Yoon, P. Westerhoff, S.A. Snyder, E.C. Wert, Nanofiltration and ultrafiltration of endocrine disrupting compounds, pharmaceuticals and personal care products, J. Membr. Sci. 270 (2006) 88–100.
[11] M. Bodzek, M. Dudziak, K. Luks-Betlej, Application of membrane techniques to water purification. Removal of phthalates, Desalination 162 (2004) 121–128.
[12] J. Cho, G. Amy, J. Pellegrino, Membrane filtration of natural organic matter: Initial comparison of rejection and flux decline characteristics with ultrafiltration and nanofiltration membranes, Water Res. 33 (1999) 2517–2526.
[13] J.L. Acero, F.J. Benitez, F. Teva, A.I. Leal, Retention of emerging micropollutants from UP water and a municipal secondary effluent by ultrafiltration and nanofiltration, Chem. Eng. J. 163 (2010) 264–272.
[14] A. Ben-David, R. Bernstein, Y. Oren, S. Belfer, C. Dosoretz, V. Freger, Facile surface modification of nanofiltration membranes to target the removal of endocrine-disrupting compounds, J. Membr. Sci. 357 (2010) 152–159.
[15] D. Dolar, A. Vuković, D.A Ašperger, K.I. Košutić, Effect of water matrices on removal of veterinary pharmaceuticals by nanofiltration and reverse osmosis membranes, J. Environ. Sci. 23 (2011) 1299–1307.
[16] K. Kimura, T. Iwase, S. Kita, Y. Watanabe, Influence of residual organic macromolecules produced in biological wastewater treatment processes on removal of pharmaceuticals by NF/RO membranes, Water Res. 43 (2009) 3751–3758.
[17] J. Wang, Synthesis and characterization of an inorganic/organic modified bentonite and its application in methyl orange water treatment, Desalin. Water Treat. 52 (2014) 7660–7672.
[18] O. Hamdaoui, C. Djelloul, Removal of cationic dye from aqueous solution using melon peel as non-conventional low-cost sorbent, Desalin. Water Treat. Sci. Eng. 52 (2014) 7701–7710.
[19] I.A.M.A. Tamer, M. Alslaibi, Kinetics and equilibrium adsorption of iron(II), lead(II) and copper(II) onto activated carbon prepared from olive stone waste, Desalin. Water Treat. Sci. Eng. 52 (2014) 7887–7897.
[20] B. Chen, C.W. Hui, M. Gordon, Pore-surface diffusion modeling for dyes from effluent on pith, Langmuir 17 (2001) 740–748.
[21] S. Wang, Y. Peng, Natural zeolites as effective adsorbents in water and wastewater treatment, Chem. Eng. J. 156 (2010) 11–24.
[22] J. Lin, Y. Zhan, Adsorption of humic acid from aqueous solution onto unmodified and surfactant-modified

chitosan/zeolite composites, Chem. Eng. J. 200–202 (2012) 202–213.
[23] R. Leyva-Ramos, A. Jacobo-Azuara, P.E. Diaz-Flores, R.M. Guerrero-Coronado, J. Mendoza-Barron, M.S. Berber-Mendoza, Adsorption of chromium(VI) from an aqueous solution on a surfactant-modified zeolite, Colloids Surf., A: Physicochem. Eng. Aspects 330 (2008) 35–41.
[24] K. Elaiopoulos, T. Perraki, E. Grigoropoulou, Monitoring the effect of hydrothermal treatments on the structure of a natural zeolite through a combined XRD, FTIR, XRF, SEM and N2-porosimetry analysis, Microporous Mesoporous Mater. 134 (2010) 29–43.
[25] C. Ortiz-Bolsico, M.J. Ruiz-Angel, M.C. García-Alvarez-Coque, Adsorption of the anionic surfactant sodium dodecyl sulfate on a C 18 column under micellar and high submicellar conditions in reversed-phase liquid chromatography, J. Sep. Sci. 38 (2015) 550–555.
[26] H. Guan, E. Bestland, C. Zhu, H. Zhu, D. Albertsdottir, J. Hutson, C.T. Simmons, M. Ginic-Markovic, X. Tao, A.V. Ellis, Variation in performance of surfactant loading and resulting nitrate removal among four selected natural zeolites, J. Hazard. Mater. 183 (2010) 616–621.
[27] H. Uslu, Adsorption equilibria of formic acid by weakly basic adsorbent Amberlite IRA-67: Equilibrium, kinetics, thermodynamic, Chem. Eng. J. 155 (2009) 320–325.
[28] Z. Aksu, E. Kabasakal, Batch adsorption of 2,4-dichlorophenoxy-acetic acid (2,4-D) from aqueous solution by granular activated carbon, Sep. Purif. Technol. 35 (2004) 223–240.
[29] M.H. Rsing, A. Ledin, R. Grabic, J. Fick, M. Tysklind, J.L.C. Jansen, H.R. Andersen, Determination of sorption of seventy-five pharmaceuticals in sewage sludge, Water Res. 45 (2011) 4470–4482.
[30] H. Yamamoto, Y. Nakamura, S. Moriguchi, Y. Nakamura, Y. Honda, I. Tamura, Y. Hirata, A. Hayashi, J. Sekizawa, Persistence and partitioning of eight selected pharmaceuticals in the aquatic environment: Laboratory photolysis, biodegradation, and sorption experiments, Water Res. 43 (2009) 351–362.
[31] T.S. Anirudhan, P.S. Suchithra, Humic acid-immobilized polymer/bentonite composite as an adsorbent for the removal of copper(II) ions from aqueous solutions and electroplating industry wastewater, J. Ind. Eng. Chem. 16 (2010) 130–139.
[32] W.S.W. Ngah, S. Fatinathan, N.A. Yosop, Isotherm and kinetic studies on the adsorption of humic acid onto chitosan-H_2SO_4 beads, Desalination 272 (2011) 293–300.
[33] A.D. Amymarie, P.M. Gschwend, Assessing the combined roles of natural organic matter and black carbon as sorbents in sediments, Environ. Sci. Technol. 36 (2002) 21–29.
[34] C.T. Chiou, D.E. Kile, D.W. Rutherford, G. Sheng, S.A. Boyd, Sorption of selected organic compounds from water to a peat soil and its humic-acid and humin fractions: Potential sources of the sorption nonlinearity, Environ. Sci. Technol. 34 (2000) 1254–1258.
[35] Q. Liu, T. Zheng, P. Wang, J. Jiang, N. Li, Adsorption isotherm, kinetic and mechanism studies of some substituted phenols on activated carbon fibers, Chem. Eng. J. 157 (2010) 348–356.
[36] J. Huang, Y. Liu, X. Wang, Selective adsorption of tannin from flavonoids by organically modified attapulgite clay, J. Hazard. Mater. 160 (2008) 382–387.
[37] R. Wang, L. Jiang, H. Wei, Z. Li, Research on mechanism of saturated zeolite regeneration, Environ. Eng. 32 (2014) 5–9.